ICARUS 28, 1–15 (1976)

Radar Observations at 3.5 and 12.6 cm Wavelength of Asteroid 433 Eros

RAYMOND F. JURGENS AND RICHARD M. GOLDSTEIN

Jet Propulsion Laboratory, Communications Systems Research Section, Pasadena, California 91103

Received August 7, 1975; revised October 6, 1975

A study of the asteroid 433 Eros using 3.5 and 12.6 cm radar waves indicates that the surface is very much rougher than any planetary or lunar surface observed by this method. A surface completely covered with sharp edges, pits, subsurface holes, or embedded chunks with scale sizes on the order of our wavelengths seems to be indicated. A model based on a rough rotating triaxial ellipsoid having radii in the rotation equator of 18.6 and 7.9 km agrees well with our data, although a strong wobble in the apparent center frequency of the spectra as rotation progresses indicates that one side may be more reflective than the other, or more likely, that the projected axis of rotation does not equally divide the projected area.

I. Introduction

The 1975 apparition of the asteroid 433 Eros was a highly unusual event from the standpoint of radar detectability. A survey of approximately 1800 asteroids indicates that this apparition of Eros is very likely to be 10 to 50 times more detectable than the next best opportunity during the following 10 years. The distance to the object is of greatest importance to the radar detectability, because the received power decreases according to the fourth power of distance. The radius of the object is of next most importance and increases the detectability according to the 3/2 power of radius for coherent radar detection. The average radius of Eros is larger than the estimated radii of most of the presently known asteroids that pass near the Earth. This, coupled with the unusually close approach, provided an opportunity to study the radar backscattering from an asteroid with much greater resolution than has been possible in the past. Although such events for the next 10 years appear less favourable, the sensitivity of radar systems will very likely increase by a factor of 10 or more during this period permitting a number of other asteroids to be studied with equal detail. Therefore, this study may be indicative of the type and quality of information that can be derived from Earth-based radar in the near future.

II. Data Acquisition

A monochromatic radar signal was transmitted toward the asteroid 433 Eros using the 64 m diameter antenna system of the Jet Propulsion Laboratory's Goldstone tracking complex. The duration of the transmitting cycle was set by the round trip time-of-flight of the radar wave, which was approximately 150 sec. This cycle was followed by a receiving period of a slightly shorter duration during which the echo was sampled, digitized, and Fourier analyzed using a Fast Fourier Transform algorithm. The power spectra were formed and accumulated for the duration of the receive cycle and recorded on magnetic tape for later processing. Following the receive cycle a third 150 sec period was used to record a signal-free

* This paper presents the results of one phase of research carried out at the Jet Propulsion Laboratory, California Institute of Technology, under Contract No. 7-100, sponsored by the National Aeronautics and Space Administration.

spectrum, which was used to remove the background from the echo spectrum. An analog filter limited the receiver bandwidth to 1400 Hz for the X-band system (wavelength of 3.53 cm) and 394 Hz for the *S*-band system (wavelength of 12.5 cm). The digital sampling was set at the Nyquist rate, and 512 contiguous samples were used in each Fourier transform. This resulted in a filter resolution of 2.73 Hz at *X*-band and 0.77 Hz at *S*-band. The maximum bandwidth expected for the target was about 500 Hz at *X*-band, and therefore the spectrum of the asteroid was resolved into more than 200 parts. The Doppler shift caused by the motion of the center of mass of the asteroid relative to the observing site was removed by a programmed local oscillator which was guided by an ephemeris which was computed by S. Pierce of the Jet Propulsion Laboratory. The entire transmit–receive–receive cycle took about 7.5 min and resulted in about 50 spectra per night of observation.

Observations were made during 7 nights, January 19 through January 26, from approximately 5 to 13 hr UT. The first and last 3 nights were used for *X*-band experiments in the polarized mode, i.e., the polarization of the receiving antenna was matched to waves having a polarization in the direction that would be expected if the target were a perfect mirror. The second night was devoted to a depolarized observation at *X*-band while the third and fourth nights were devoted to polarized and depolarized observations at *S*-band, respectively.

Because the measurement of radar cross section was essential to this experiment, considerable attention was given to the problems of calibration of the transmitted power, the antenna gain, atmospheric absorption, and the receiver system temperature. The prime calibration of the transmitter is accomplished by connecting a dummy load to the output port. The dummy load is cooled by pumping water through the load, and the flow rate and temperature difference of the water are accurately measured to determine the total power dissipated in the load. This measurement is then used to calibrate an electrical power output meter. The calibration of the receiver system is accomplished by measuring the temperature difference between two dummy loads connected to the input port of the receiver system. The loads are maintained at room and liquid-nitrogen temperatures and serve as a prime calibration source. The prime standard is used to calibrate a gas tube noise source which is injected into the input port of the receiver system. The gas tube system then serves as a secondary calibration standard and is used for all calibration during the radar observations. The effective collecting area and gain of the antenna system is calibrated by measuring the power collected when a number of radio star calibration sources are tracked. The radio fluxes of calibration sources have been measured using calibration horn antennas having accurately known apertures. These data were used to determine the efficiency of the aperture relative to the geometric area as a function of elevation angle. During the observations the transmitted power was recorded for each transmit cycle, and receiver calibration was carried out at the beginning and end of each observation, and hourly. Two temperature calibration points were measured with the antenna at zenith in order to aid in measuring atmospheric absorption and noise contribution. These data were used to determine a temperature calibration curve that was dependent on the secant of the zenith angle. Corrections were made for variations in the effective antenna gain caused by deformation of the surface structure and for absorption due to the neutral atmosphere. These corrections were particularly important to the *X*-band sensitivity calibration. The absolute calibration of the *S*-band system is believed to be ± 0.6 db while the absolute calibration of the *X*-band system is presently less certain. Accurate pointing corrections for the *X*-band system are not yet available. A decrease in radar cross section for the last day of observation is believed to be due to pointing inaccuracies.

All frequency and time standards were derived from the station master clock.

which has a hydrogen maser as a prime reference. This system is stable to about 1 part in 10^{14}.

III. Analysis

Average Properties (Full Rotation Period)

The average properties of the asteroid were measured by preparing a weighted average of the power spectra for one full rotation period of 5.268912 hr as measured optically by Dunlap (1975).[1] The weights were chosen to compensate for variations in system sensitivity so as to maximize the signal-to-noise ratio, as opposed to establishing uniform sampling over the full rotation period. As a result some rotation phases may be represented somewhat more strongly than others in the average. The resulting spectra showed no strong central peak as is usually associated with the quasi-specular backscattering characteristic of lunar and planetary radar spectra. Figure 1 shows 3 spectra typical of planetary radar targets for comparison with the spectrum of Eros. The lowest curve shows a spectrum of Mercury made in the polarized mode while the next above it is a spectrum in the cross polarized mode. The large difference in spectral shape is characteristic of lunar and planetary targets. The third graph from the bottom shows a spectrum of Venus in the cross polarized mode. The anomalous bumps (features) are clearly evident, and are not observed in the radar spectra of Eros. The uppermost curve is, of course, the average spectrum of Eros made in the polarized mode, and because of the

[1] The first prime minimum of January 19, 1975, occurs at 01:40, corresponding to a total angle of rotation from 0.0 Hr of 113°8755.

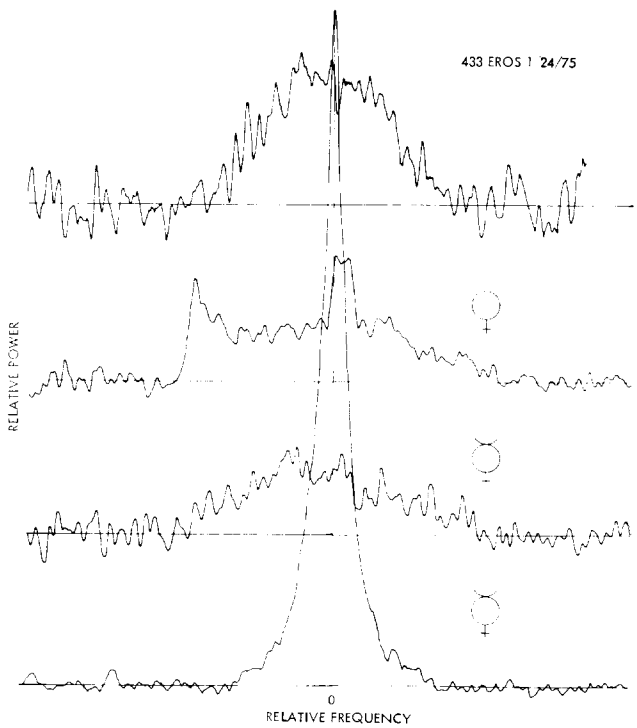

FIG. 1. Average radar spectrum of Eros in the polarized mode compared to radar spectra of Mercury and Venus. The lowest graph shows a spectrum of Mercury in the polarized mode while the curve above shows the cross polarized mode. The third curve up from the bottom shows a cross polarized spectrum of Venus. All power and frequency units are arbitrary.

averaging over a full rotation period no features would be evident. The spectral shape appears to be more like the cross polarized planetary spectra than the polarized spectra. Such spectral shapes appear similar to those of spherical radar targets having a backscattering function, $S(\theta)$, of the form $\cos^n\theta$ where θ is the angle between the observer and the normal to the surface and n is a number near 2. This scattering model was chosen for initial data processing.

The power spectrum, $P(f)$, from such a model can be shown to be

$$P(f) \sim \begin{cases} [1 - ((f-f_0)/f_m)^2]^{n/2}, & |f-f_0| \leq f_m \\ 0, & \text{elsewhere,} \end{cases}$$

where f_m is the maximum frequency at the limb (one-half of the limb-to-limb bandwidth), f_0 is the center frequency, and $n > -1$ (e.g., see Goldstein, 1964). The method of nonlinear least-squares regression was used to determine the free amplitude parameter, f_0 and f_m. Since any single night of operation gave a data span slightly less than 8 hr, roughly one and a half rotations were observed. Two averages were constructed from each night's observation by using the first 5.27 hr of data in the first average and then forming a second average 2.64 hr later. The second average seldom contained a full 5.27 hr of data, and obviously the resulting measurements are not independent but do give some feeling for the measurement errors to compare with the formal error estimates.

Table I shows the measured values of radar cross section in meters squared and the half-bandwidth in Hertz. The data were processed for values of $n = 1$, 2, and 4, and the tabulated measurements are for $n = 2$. Increased values of n cause larger apparent bandwidths and better convergence of the iteration process with little difference in the total rms error. Estimates of the radar cross section were prepared from both the model spectra, σ_m, and directly from the observed power spectra, σ_d. These numbers agreed within the formal error estimates in all cases, indicating that no worthwhile systematic errors were present.

Certain conclusions about the properties of the surface of the asteroid can be drawn directly from the measurements of Table I. Most interesting is the fact that no significant difference exists between the bandwidths of the X-band spectra when the receiving antenna is set for either sense of circular polarization. This indicates that the spectral shapes, and therefore the scattering laws, are nearly identical in either polarization. Furthermore, if the ratio of the bandwidths of the polarized spectra at X-band to S-band are calculated ($f_{mx} \cong 305$, $f_{ms} \cong 82$ Hz) a value of 3.72 is found. This bandwidth ratio is only slightly larger than the ratio of the transmitter frequencies (8495 to 2388 MHz) which is 3.56, and indicates that the scattering laws for the two wavelengths are almost identical and that surface must be sufficiently rough that the increase

TABLE I

SUMMARY OF RADAR CROSS SECTIONS AND APPARENT CENTER TO LIMB BANDWIDTHS BASED ON SPECTRA AVERAGED OVER APPROXIMATELY ONE ROTATION PERIOD (FORMAL ERRORS, 1σ)

Date	Band	Polarization	Cross section (m^2)	Bandwidth f_m (Hz)
Jan. 19, 1975	X	P	$(2.99 \pm 0.12) \times 10^7$	334 ± 11
Jan. 20, 1975	X	CP	$(8.48 \pm 0.93) \times 10^6$	313 ± 29
Jan. 22, 1975	S	P	$(3.84 \pm 0.34) \times 10^7$	82 ± 6
Jan. 23, 1975	S	CP	$(8.40 \pm 5.8) \times 10^6$	68 ± 21
Jan. 24, 1975	X	P	$(2.34 \pm 0.08) \times 10^7$	287 ± 8
Jan. 25, 1975	X	P	$(2.29 \pm 0.07) \times 10^7$	309 ± 7
Jan. 26, 1975	X	P	$(1.25 \pm 0.06) \times 10^7$	307 ± 2

in wavelength by 3.5 times has little effect on the backscattering mechanism.

The backscattering law is believed to be associated with the depolarized or diffuse component is of the form $S(\theta) \sim \cos^n(\theta)$ where n is 1 or 2 (e.g. see Evans and Hagfors, 1966; Renau *et al.*, 1967; and Fung, 1967). It would appear that the backscattered power from a surface as rough as indicated by the above measurements should be equally distributed in either polarization. Such is not the case. The ratios of polarized radar cross section to depolarized is about 3 at X-band and roughly 4 at S-band. The depolarized measurement at S-band is sufficiently poor that ratios between 2 and 16 are possible. Therefore, it is not possible to establish whether the surface is less diffuse at the longer wavelength.

The deduction of further physical parameters for the asteroid from the averaged spectra requires certain assumptions that can be eliminated by more refined analysis of the spectra averaged over much shorter periods. However, interpretations of radar measurements of bandwidth and cross section are traditional, and it is interesting to see what results can be obtained using the usual assumptions. In particular, the mean radius of the asteroid can be estimated from the bandwidth of the echo or the radar cross section. Assumptions concerning direction of the polar axis, the form of the scattering law, and the effect of averaging spectra from an irregularly shaped object must be considered in the case of bandwidth. The half bandwidth, f_m, is given by

$$f_m = (2\Omega R/\lambda)\cos\delta,$$

where Ω is the rotation rate, R is the radius, λ is the wavelength of the radar system, and δ is the declination of the Earth as measured from a coordinate frame centered on the asteroid. δ is known to be near 20° at the time of our observations from the measurement of Dunlap (1976). From the bandwidth data the largest radius must be greater than 17 km. The estimates of f_m increase when the observations are processed with larger values of n in the scattering law, yielding even larger radii. The effect of other assumptions is unknown.

The radar cross section is given by $\sigma = \pi R^2 \rho g$, where ρ is the efficiency coefficient of the surface material and g is a surface gain coefficient associated with the backscattering directivity. The mean radius can be calculated from the cross section formula if some assumptions can be made about the product ρg. A value of ρg near 0.1 is typical of many planetary and lunar surfaces, but all planetary and lunar surfaces observed so far exhibit highly quasi-specular backscattering characteristics which have values of the gain coefficient near unity. Radar measurements of Icarus and Toro reported by Goldstein (1968, 1969 and by Goldstein *et al.* (1973) indicate that very rough surfaces may be characteristic of small asteroids. A very rough surface exhibiting a Lambert scattering characteristic might have a gain as large as 4/3 if only one polarization is observed. Other scattering models could be assumed. For example, Muhleman's quasi-specular model based on a faceted surface reduces to $S(\theta) \sim \cos\theta$ when the roughness parameter is set to unity, and gives a surface gain of 3/2 (e.g., see Muhleman, 1964, 1966). Greater variations might be expected in ρ. Table II shows the values of mean radius based on various assumptions for ρ and g. These radii are all much smaller than indicated by the bandwidth measurement. This discrepancy could indicate that the reflectivity of the surface material is smaller than any of the assumed values or that the largest radius in the rotation plane

TABLE II

MEAN RADII BASED RADAR CROSS SECTION DATA FOR SEVERAL ASSUMPTIONS OF SURFACE REFLECTIVITY AND BACKSCATTER GAIN

	Moon $\rho = 0.08$	Venus $\rho = 0.15$	Solid iron $\rho = 1.0$
Lambert $g = 4/3$	8.4	6.2	2.4
Muhleman $g = 3/2$	8.0	5.8	2.3

is dominant in establishing the bandwidth of the average spectrum.

Averages Over Shorter Time Spans

In order to achieve finer time resolution, the fitting procedure described in the previous section was applied to individual X-band spectra (2.5 min average), spectra averaged for one-half hour duration, and spectra averaged for one quarter of a rotation period. Of these, the one-half hour averages seem to present the best compromise between time resolution and adequate signal to noise ratio. Radar cross section, center frequency, and bandwidth were estimated as before, and these data are shown in Figs. 1 through 4. Average spectra were prepared for time steps of 15 min; therefore adjacent measurements are not independent, but a smoother curve results. The amplitude of the spectra taken on the last day (January 26, 1975) were increased by a factor of 1.78 to compensate for the apparent pointing error on this date.

Figures 1 through 4 show that the bandwidths near the times of prime minima average about 200 Hz while values of 350 Hz are typical near the maxima. The values of cross section average about $1 \times 10^7 \text{m}^2$ near the prime minima and about $3.5 \times 10^7 \text{m}^2$ near the maxima. If the scattering law of the asteroid were proportional to $\cos^1\theta$, the radar cross section would be proportional to the projected area, and the ratio of σ_{max} to σ_{min} would give a good estimate of the ratio of the lengths of the two axes in the rotation equator if δ is not too large. If the exponent of the cosine scattering law is larger than one, the cross section ratio would be larger than the length ratio of the two axes. The bandwidth ratio is also a sensitive indicator of the ratio of lengths of the axes in the rotation equator and is independent of δ if the scattering law is $\cos^1\theta$. The bandwidth ratio also increases with an increase in the exponent of the cosine scattering law, but not so rapidly as the radar cross section. The measured ratios of cross section and bandwidth are probably smaller than would be observed if the rather sharp minima were not smeared out by the averaging process.

The solid curves shown in Figs. 2–5 are Fourier series representations of the measurements using only a constant,

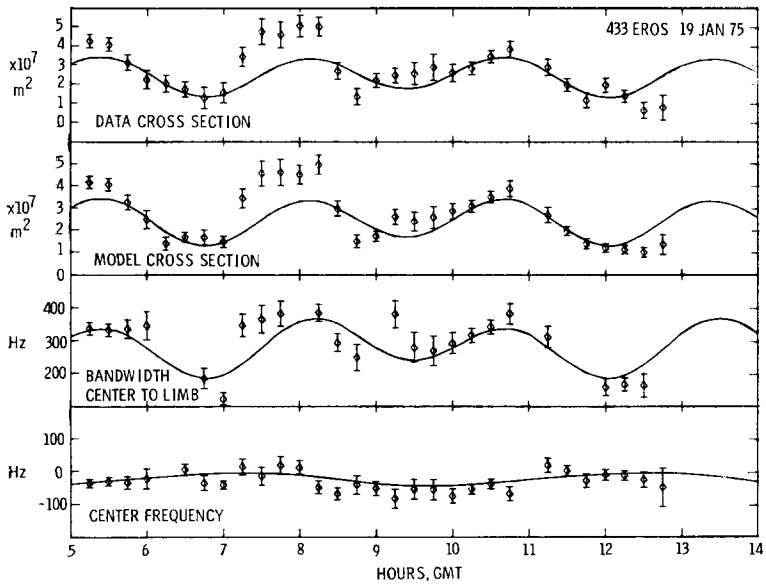

FIG. 2. Measurements of center frequency, bandwidth, and radar cross section for observations of January 19, 1975.

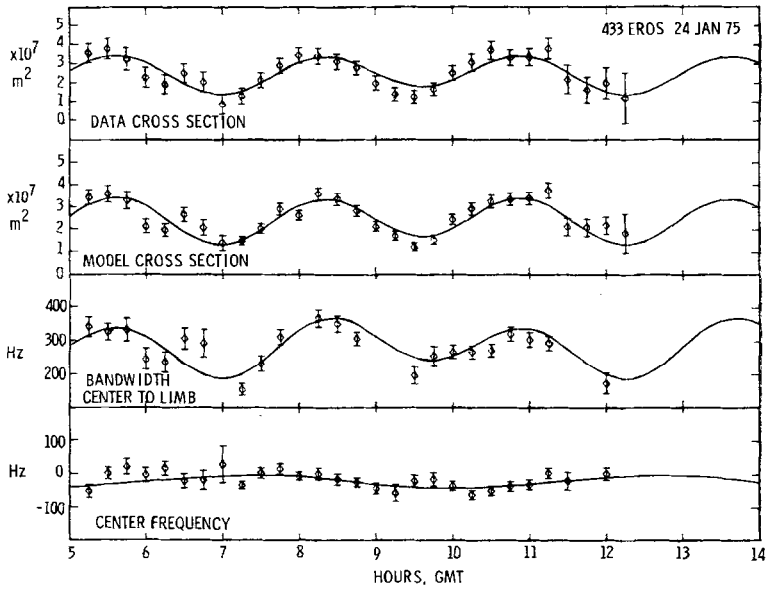

FIG. 3. Measurements of center frequency, bandwidth, and radar cross section for observations of January 24, 1975.

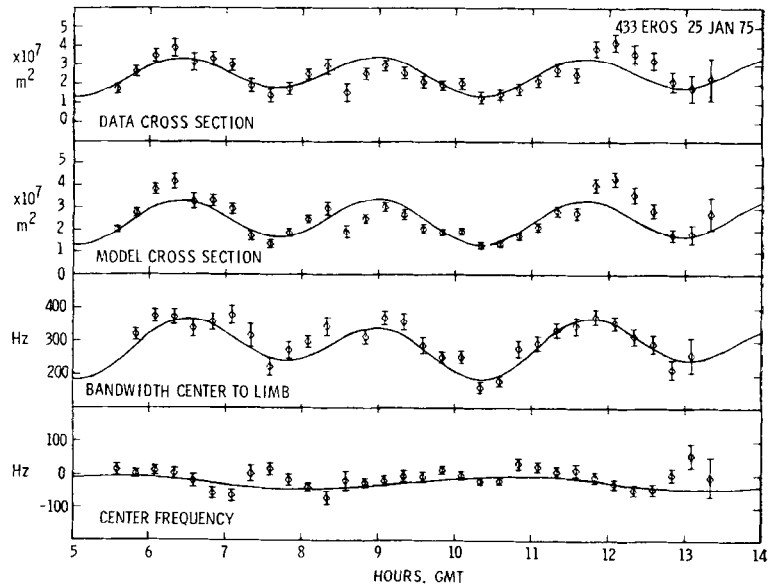

FIG. 4. Measurements of center frequency, bandwidth, and radar cross section for observations of January 25, 1975.

fundamental, and second harmonic terms. The Fourier series for the center frequency, bandwidth, and model radar cross section are given, respectively, by

$$f_0 = (-10.0 \pm 2.5)\cos\Omega t + (16.4 \pm 2.7)\sin\Omega t + (1.9 \pm 2.6)\cos 2\Omega t + (-0.1 \pm 2.6)\sin 2\Omega t, \quad (1)$$

$$f_m = (283.8 \pm 2.8) + (-7.2 \pm 3.7)\cos\Omega t + (-31.5 \pm 4.1)\sin\Omega t + (61.2 \pm 4.0)\cos 2\Omega t + (35.1 \pm 3.9)\sin 2\Omega t, \quad (2)$$

$$\sigma_m = 10^6\{(24.3 \pm 0.30) + (0.72 \pm 0.39)\cos\Omega t + (-1.79 \pm 0.35)\sin\Omega t + (8.9 \pm 0.36)\cos 2\Omega t + (3.7 \pm 0.37)\sin 2\Omega t\}, \quad (3)$$

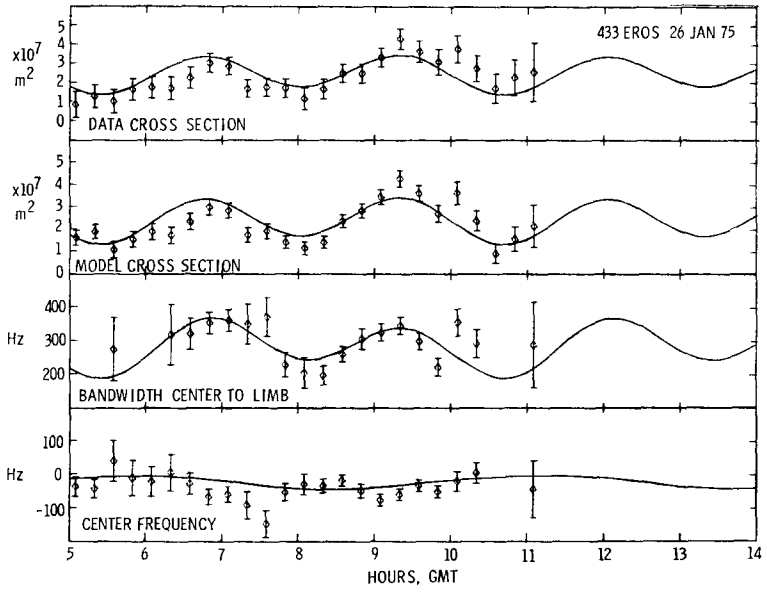

FIG. 5. Measurements of center frequency, bandwidth, and radar cross section for observations of January 26, 1975 with radar cross section data rescaled to match the average radar cross section of Figs. 1 through 3.

where Ω is $2\pi/5.268912$ and time, t, in hr is referenced to 0.0 Hr UT on January 19, 1975. Of particular interest is the wobble in center frequency, which has a strong fundamental component but no significant second harmonic. A rotating triaxial ellipsoid, for example, having axes $a = 18 \times 10^3$, $b = 6 \times 10^3$, and $c = 6 \times 10^3$ m, $\delta = 20°$, and the exponent of the scattering law, n, equal to 2 would exhibit a ± 15 Hz wobble every half revolution. If $n = 1$, no wobble would be observed. The absence of the detection of this component may mean that the value of n is near unity. If this is the case, the strong fundamental term must be attributed either to variations in surface reflectivity from one side to the other or to varing amounts of projected area either side of the projected axis of rotation. The second possibility is most likely the case, since no optical differences in either color or polarization characteristics were observed during rotation by Miner and Young (1976), or Zellner and Gradie (1976).

Some fundamental component also exists in the Fourier series for the bandwidth and radar cross section. This term is probably introduced by differing amounts of bluntness when the asteroid is oriented to minimum projected area.

The depolarized X-band observations as well as the S-band polarized and depolarized observations were processed in the same way as described above. Although these data are sufficiently poor that the center frequency and bandwidth cannot be measured in many cases, the radar cross section can be measured. In particular, the measurements of the radar cross section at the times of the maxima are of fairly good quality and a good estimate of the depolarized X-band cross section is 1.25×10^7 m^2. This would give a ratio of σ_P/σ_D of 3 to 1. A somewhat improved ratio for the S-band observations can be obtained in the same manner using the radar cross sections at the prime maxima. The results are $\sigma_P = (8.0 \pm 1.4) \times 10^7$ and $\sigma_D = (3.0 \pm 1.4) \times 10^7$ m^2. The ratio σ_P/σ_D would be $2.7^{+3.2}_{-1.2}$. These ratios are not very different from those found from the full period averages though they are based on radar cross section measurements that are larger than those from the full period averages.

Averages Over Constant Phase

Because the measurement of the minimum bandwidth is difficult to make with the previous procedure, we organized the spectra of the last three consecutive days into sixteen bins of nearly constant rotation phase. The first phase bin is centered at 0.0 Hr UT on January 19, 1975, and the time separation of each bin thereafter is given by the rotation period divided by sixteen. Therefore, the smearing in time or phase angle is about 20 min or 22.5° and offers some improvement over the previous procedure. The variation in the angle of the observer above the rotation plane is only a few degrees over the span of the observations, and no significant smearing of the spectra is expected due to this variation. The main danger of this procedure is that the Doppler frequency of the center of mass may have drifted relative to the Doppler frequency of the trial ephemeris. The largest Doppler frequency drift appears to be associated with the observations on the final day, which happens to be weighted down by a factor of three due to the pointing problem. We believe that the effective smearing of the spectra is less than 20 Hz, i.e., the bandwidth of the spectra should not be widened by more than 20 Hz due to center frequency drift over the 3 days of observation. The minimum bandwidth expected is probably not less than 100 Hz, and therefore the drift is not entirely insignificant. The resulting sixteen spectra are shown in Fig. 6.

Although the exact shape of the spectra cannot be determined, some of the general features such as width, average flatness, and approximate center can be discerned by sketching average curves through the plots. The intensity near the center of the spectra remains fairly constant for each phase, and only the widths seem to vary. Spectrum number six falls near the time of a prime minimum and can be seen to be the narrowest. Actual measurements of center frequency, bandwidth and radar cross section have been made using the modeling procedure discussed earlier. The results of this analysis are shown in Fig. 7. The solid curves are Fourier series representation of the data, and the series are by

$$f_0 = (-9.5 \pm 3.0)\cos\Omega t + (2.2 \pm 3.0)\sin\Omega t + (5.3 \pm 3.0)\cos 2\Omega t + (1.8 \pm 3.0)\sin 2\Omega t, \quad (4)$$

$$f_m = (276 \pm 3) + (10.7 \pm 4.4)\cos\Omega t + (-2.3 \pm 4.4)\sin\Omega t + (72.5 \pm 4.3)\cos 2\Omega t + (44.2 \pm 4.5)\sin 2\Omega t, \quad (5)$$

$$\sigma_m = 10^6\,[(23.5 \pm 0.3) + (0.67 \pm 0.45)\cos\Omega t + (-1.00 \pm 40)\sin\Omega t + (8.59 \pm 0.43)\cos 2\Omega t + (5.09 \pm 0.42)\sin 2\Omega t]. \quad (6)$$

The bandwidth of spectrum six is 167 Hz and spectrum number nine has the largest width of 359 Hz, giving a bandwidth ratio of 2.15. The ratio of maximum to minimum radar cross section is approximately 2.56, with spectrum six exhibiting the smallest radar cross section of 1.29×10^7 m^2. If we subtract approximately 20 Hz from the smallest bandwidth measurement to compensate for possible smearing, the bandwidth ratio is increased only to 2.44. In that case the bandwidth ratio is nearly equal to the radar cross section and a value of n approaching unity would be indicated.

The Fourier analysis of the center frequency data indicates a strong wobble at the fundamental rotation frequency and a nearly insignificant second harmonic term. From the standpoint of further analysis of the Eros observations it is important to note that the center frequency variation reaches its maximum and minimum values near the times of minima of the light curves and correspondingly with the minima of bandwidth and cross section curves. These data again seem to indicate that the ratio of the axes in the rotation equator is less than 2.5 to 1, although the ratios of maximum to minimum values of bandwidth and radar cross section could be somewhat larger due to the fact that the smearing over 22°.5 in phase has not been taken into account.

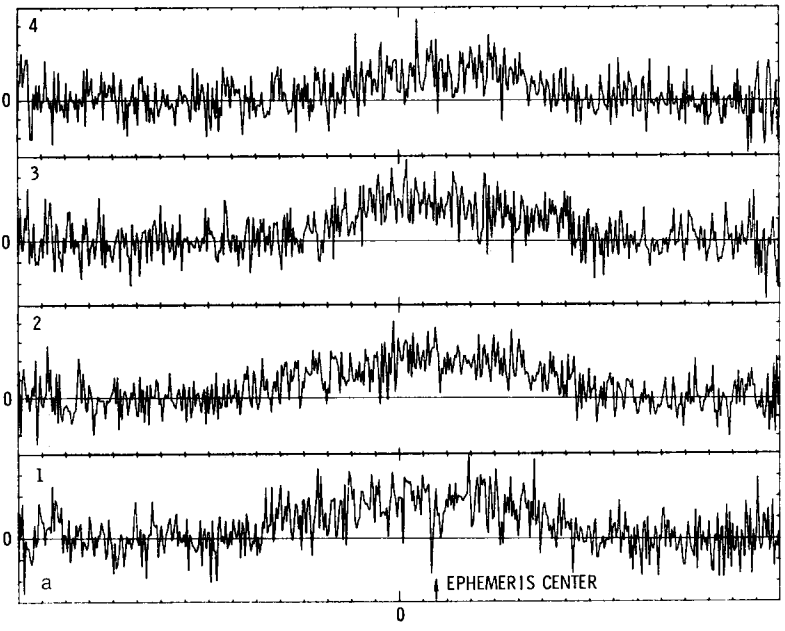
4
0
3
0
2
0
1
0
a
EPHEMERIS CENTER
0

FIG. 6(a)

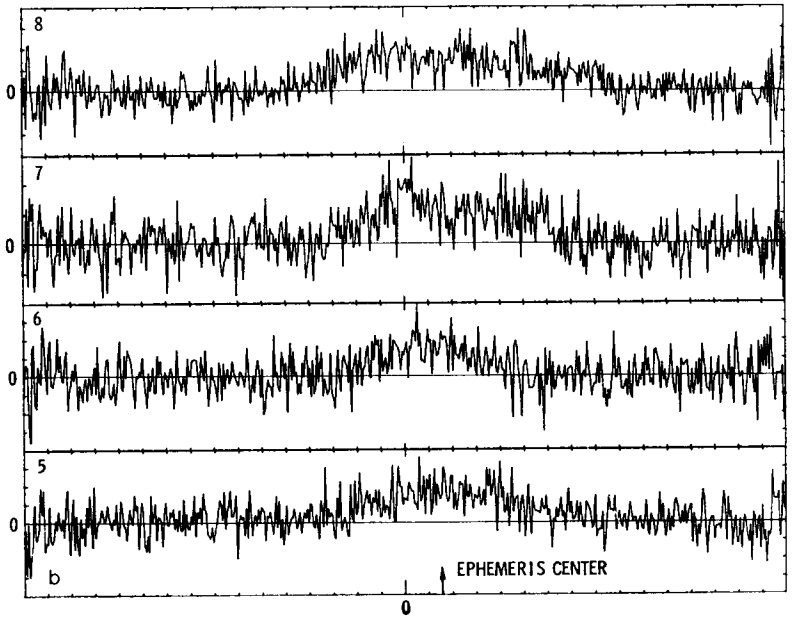
8
0
7
0
6
0
5
0
b
EPHEMERIS CENTER
0

FIG. 6(b)

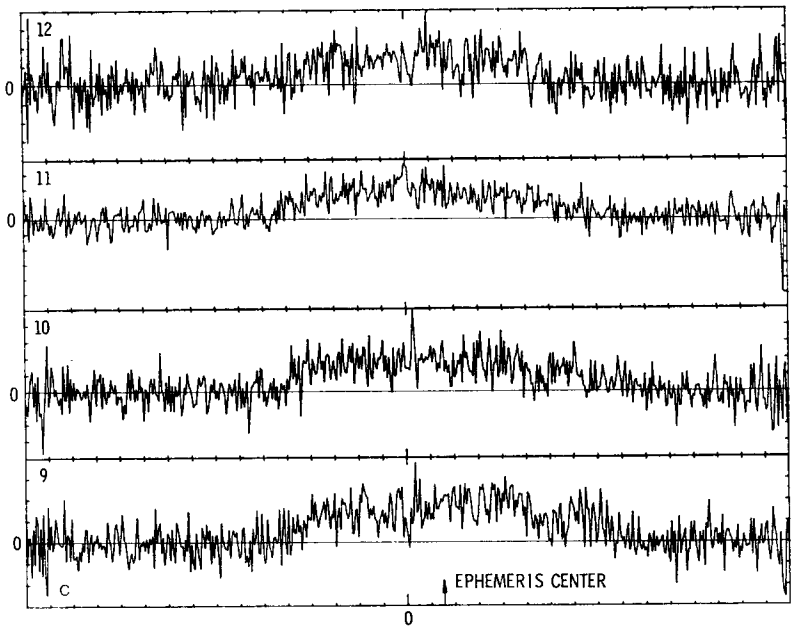

FIG. 6(c)

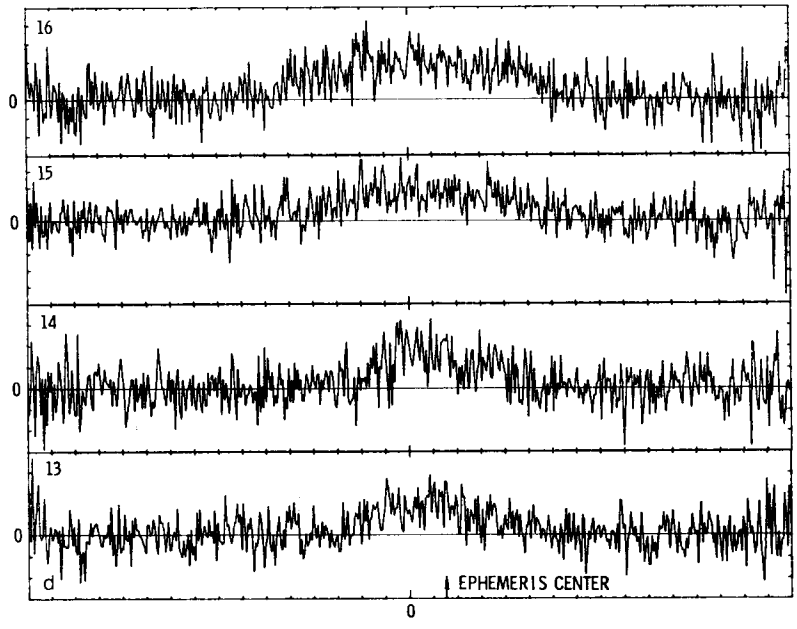

FIG. 6(d)

FIG. 6. X-Band polarized observations of January 24, 25 and 26, 1975, averaged into bins of rotation phase of width 22°.5. The first bin is centered at 0.0Hr UT on January 19, 1975. The vertical scale is area per filter resolution cell; the vertical ticks are $1.0 \times 10^5 m^2$ per filter width, and the horizontal ticks are every 16 resolution cells.

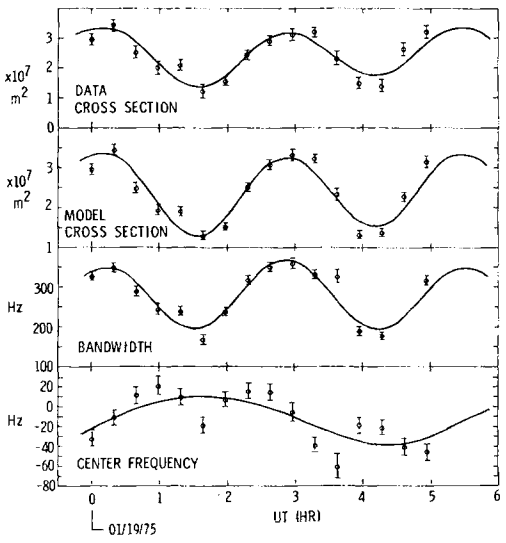

FIG. 7. Measurements of center frequency, bandwidth, and radar cross section from spectra averaged into sixteen phase slots.

Modeling with a Triaxial Ellipsoid

In order to avoid the smearing problem associated with time and phase averages and to eliminate the convergence problems associated with fitting spectra models to noisy radar spectra containing a small number of points, we have fit a model based on a rough rotating triaxial ellipsoid to the X-band polarized spectra of January 24 and 25, 1975. The model contains 9 parameters, which are the reflection coefficient, the center frequency, the lengths of three axes, the angle of the observer above the rotation plane, a rotation phase angle, the rotation rate and the exponent of the cosine scattering law, giving a vector of unknowns $(\rho, f_0, a, b, c, \delta, \psi, \Omega, n)$, respectively. We considered the rotation rate Ω to be known and constructed a correlation matrix of the remaining 8 parameters to determine the correlations and formal errors associated with the solution of various remaining subsets of the parameters. A strong correlation between the length along the spin axis, c, and the reflection coefficient made it impossible to determine these independently. A strong correlation also existed between the angle, δ, and the two lengths of the axes in the rotation equator. Although the rotation phase angle, ψ, was well determined, the optical measurement of the times of prime minima established a better estimate of this parameter. As pointed out earlier, adjacent minima correspond to opposite center-frequency shifts. We have chosen to remove the fundamental component of frequency shift as well as daily frequency offsets using the estimates from the first two procedures rather than attempt to simultaneously fit a larger set of parameters to account for the motion of the center frequency. Four free parameters (ρ, a, b, n) were adjusted to minimize the mean-square error between the data set and the computed spectral density based on the model.

Table III lists the assumed values of various parameters which have been fixed. The 7×10^3 m value assumed for the third axis is simply a guess. The major effect of increasing the size of this axis is to decrease the reflection coefficient proportionally, thus the assumption is not too critical except to the interpretation of the surface reflectivity.

TABLE III

SUMMARY OF FORCED PARAMETERS USED TO ESTIMATE THE FREE PARAMETERS

Parameter	Assumed value	Comment
f_0	$-17.9 + 24.1\cos(\Omega t - 113.1)$	For data of Jan. 24, 1975
f_0	$-5.0 + 24.1\cos(\Omega t - 113.1)$	For data of Jan. 25, 1975
c	7.0×10^3m	
δ	20.0	Dunlap, 1976
ψ	113.875	Dunlap, 1975
Ω	$2\pi/5.268912$ radians per hour	Dunlap, 1976

TABLE IV

MEAN VALUES, STANDARD ERRORS, AND CORRELATION MATRIX FOR REDUCTION WITH ρ, a, b, and n as FREE PARAMETERS

	ρ	a (m)	b (m)	n
	0.123	19.16×10^3	11.39×10^3	2.447
ρ	0.0066			
a	0.3852	0.205×10^3		
b	0.7638	0.3494	0.376×10^3	
n	0.9766	0.4462	0.8131	0.170

Table IV shows the results of a four parameter solution using the assumed values of Table III. The values of ρ, a, b, and n are given with the formal errors along the diagonal of the matrix and the normalized correlation coefficients presented in the off-diagonal locations. The correlations between ρ and n and between b and n are larger than we anticipated, and the value of n is larger than thought to be possible since the center frequency excursion for this model would be ± 16 Hz and should be observable, unless by some chance the same mechanism that generates the wobble in center frequency at the fundamental frequency of rotation also generates a term at the second harmonic frequency which has both the proper amplitude and phase to cancel out the wobble generated by that part of the figure that is recurrent every half rotation. This seems unlikely. Therefore we have fixed the value of n to 1.2, which results in a frequency wobble about equal to our detection threshold. Table V shows the results of the three-parameter solution. The most important difference is that the length of the small axis has been reduced by 2.6 km.

TABLE V

MEAN VALUES, STANDARD ERRORS, AND CORRELATION MATRIX FOR REDUCTION WITH $n = 1.2$ and ρ, a, and b as FREE PARAMETERS

	ρ	n	b (m)
	0.0780	18.41×10^3	8.775×10^3
ρ	0.00094		
a	−0.1970	0.157×10^3	
b	−0.2829	−0.2936	0.151×10^3

The light intensity scattered from Eros varies by a factor of 4 to 1 during a rotation, and one might infer that a ratio of the axes in the rotation equator is equally large. The analysis by Dunlap (1976), however, gives a ratio of about 3 to 1 when the effect of shadowing is taken into account. Since this ratio is larger than ours, and because most of the systematic errors in estimates of the other parameters would tend to reduce the ratio which we estimate, we have explored the possibility that certain of our assumptions are in error. In particular, we have assumed that the minimum radar cross section does not occur in synchronism with the minima of the light curves. The Fourier series representation of our bandwidth and radar cross section data given in (2), (3), (5), and (6) all give minima that occur about 10 min earlier than the first prime minimum after 0.0 Ht UT on January 19, 1975. Therefore, we included the phase reference angle, ψ, as a free parameter. The results are shown in Table VI. Here ψ has been reduced to $102.1 \pm 0.7°$ and the small axis by roughly 1 km. The phase difference would indicate that the time of prime minimum reflected back from the data of January 24–26, 1975, to the nearest prime minimum following 0.0 Hr UT on January 19, 1975, is 10.36 min prior to the time of the first optical prime minimum of that date.

The data of Table VI yield a model that is in good agreement with the direct

TABLE VI

MEAN VALUES, STANDARD ERRORS, AND CORRELATION MATRIX WITH ψ_0 INCLUDED AS A FREE PARAMETER

	ρ	a (m)	b (m)	ψ
	0.0804	18.58×10^3	7.87×10^3	102.1
ρ	0.00096			
a	−0.1934	0.150×10^3		
b	−0.2938	−0.2843	0.150×10^3	
ψ	−0.0066	0.0311	0.0223	0.690

measurements of center frequency, bandwidth, and radar cross section as well as ratios prepared from these. The center frequency wobble is about ±3 Hz, which is just below our detection threshold, while the maximum and minimum values of bandwidth are 364.3 and 150.2 Hz, giving a ratio of 2.42. The maximum and minimum values for the radar cross section are 3.08×10^7 and 1.48×10^7 m^2 giving a ratio of 2.07. The actual ratio of the two axes in the rotation equator is 2.36.

The meaning of our reflection coefficient, ρ, is different from the usual meaning where ρ is the Fresnel reflection coefficient associated with the reflection from a dieletric interface. In our case, ρ is simply the multiplier of the $\cos^n\theta$ scattering function required to cause the spectral density of the model to match the measured spectral density. The connection of this parameter to physical parameters of the surface requires information about the forward scattering properties of the surface as well as the ability to model the depolarizing mechanism which contributes extensively to both the polarized and depolarized radar cross section.

IV. CONCLUSIONS

The results of this study indicate that the surface of Eros in exceedingly rough. A surface completely filled with sharp edges, pits, subsurface holes or chunks of imbedded material would be in good agreement with our data.

Analysis of the curves of center frequency, spectrum bandwidths, and radar cross section as a function of time or rotation phase indicate that the ratio of radii in the rotation equator must be near 2.5 to 1. Model spectra generated from a rotating triaxial ellipsoid are in good agreement with our measured spectra if the radii in the rotation equator are 18.6 and 7.9 km. A backscattering function of the form of $\cos^n\theta$ is indicated where $1 \leqslant n < 1.5$ for the polarized component and not greatly different for the depolarized component, though direct measurement is not possible with our data.

A strong wobble in the apparent center frequency of the spectra is observed as rotation progresses. This component of the wobble is periodic in the rotation frequency of the asteroid and contains no measurable second harmonic. The peak excursions in center frequency occur at the times of minimum radar cross section and spectral width. The expected center frequency of a rotating triaxial ellipse would be zero at these times. Therefore, this component must be generated by some asymmetry in the figure, a denser material on one side or the other, or by a difference in surface reflectivity or surface slopes on opposite sides of the asteroid.

REFERENCES

DUNLAP, L. (1976). Light curves and the axis of rotation of 433 Eros. *Icarus* **28**, 69–78.

DUNLAP, L. (1975). Private communication.

EVANS, J. V., AND HAGFORS, T. (1966). Study of radio echoes from the Moon at 23 centimeters wavelength. *J. Geophys. Res.* **71**, 4871–4889.

FUNG, A. K. (1967). Characteristics of wave polarizations by perfectly conducting rough surface and its application to Earth and Moon experiments. *Planet. Space Sci.* **15**, 1337–47.

GOLDSTEIN, R. M. (1964). Venus characteristics by Earth-based radar. *Astron. J.* **69**, 14.

GOLDSTEIN, R. M. (1968). Radar observations of Icarus. *Science* **162**, 903–904.

GOLDSTEIN, R. M. (1969). Radar observations of Icarus. *Icarus* **10**, 430–431.

GOLDSTEIN, R. M., HOLDRIDGE, D. B., AND LIESKE, J. H. (1973). Minor planets and related objects. XII. Radar observations of (1685) Toro, *Astron. J.* **78**, 508–509.

MINER, E., AND YOUNG, J. (1976). Five color photoelectric photometry of asteroid 433 Eros. *Icarus* **28**, 43–51.

MUHLEMAN, D. O. (1964). Radar scattering from Venus and the Moon. *Astron. J.* **69**, 34–41.

MUHLEMAN, D. O. (1966). Planetary characteristics from radar observations. *Space Sci. Rev.* **6**, 341–364.

RENAU, J., CHEO, P. K., AND COOPER, H. G. (1967). Depolarization of linearily polarized EM waves backscattered from rough metals and inhomogeneous dielectrics. *J. Opt. Soc. Am.* **57**, 459–466.

ZELLNER, B., AND GRADIE, J. (1976). Polarization of the reflected light of asteroid 433 Eros. *Icarus* **28**, 117–123.